MEASURING GROUND SUBSIDENCE IN SHANGHAI USING PERMANENT SCATTERER INSAR TECHNIQUE

P. Damoah-Afari
Department of Land Surveying and Geo-Informatics
Hong Kong Polytechnic University
Hong Kong
p.damoah@polyu.edu.hk

X.L. Ding
Department of Land Surveying and Geo-Informatics
Hong Kong Polytechnic University
Hong Kong
lsxlding@polyu.edu.hk

Abstract: The city of Shanghai has been experiencing subsidence since 1921 mainly due to intensive withdrawal of water from underground [1][2], and to some extent due to rapid infrastructural developments taking place in the city (e.g., concentration of skyscrapers in Xuhui District and the Lujiazui Financial Zone of the Pudong District) [3]. Subsidence phenomenon in Shanghai has been previously measured or monitored using the surveyor's method of precise leveling, and more recently the global positioning system (GPS). Although these methods provide precise measurements they are labour and time intensive, costly and are restricted to specific points in the terrain. Inteferometric synthetic aperture radar (InSAR) has demonstrated the capability of mapping extensive areas, on pixel-by-pixel basis, and in a more convenient manner than the aforementioned geodetic methods. In this paper, the strength of using the permanent scatterer (PS) InSAR technique, an advanced form of the conventional differential InSAR technique, is used for measuring ground subsidence in Shanghai. Nineteen (19) ERS-1 and ERS-2 SAR single look complex (SLC) scenes acquired over Shanghai during the period 6 June 1992 – 20 November 2001 were used for the study. The images have a maximum relative temporal baseline of 3454 days (approximately 9.5 years) and a minimum relative temporal baseline of 1 day. Over 21000 PS were extracted, and preliminary result is in sympathy with some reported studies, as well as the reported annual average subsidence rates based on precise leveling and global positioning systems (GPS) surveys over well established benchmarks in the city.
Keywords: Land Subsidence, Permanent Scatterer InSAR, Differential InSAR, InSAR, Deformation.

Introduction

Owing to natural causes and human activities, the ground that supports all features, including humans, is in motion at some locations on the Earth's surface. Human factors such as intensive withdrawal of water and petroleum, and removal of precious minerals from underground have resulted in severe subsidence in many parts of the world. Engineering facilities on the ground surface (e.g., buildings, roads and bridges) and underground (e.g., tunnels, drainage and sewage systems) are the most affected in this process.

Shanghai, one of the world's megacities, is experiencing subsidence mainly due to anthropogenic factors – intensive exploitation of ground water and the construction of high-rise buildings. It is estimated that the high-rise buildings contribute about 30 to 40 per cent (30 – 40 %) of the subsidence problem [3], and that withdrawal of water from underground, however, remains the main cause of subsidence in Shanghai [1][2]. In their report on land subsidence in Shanghai, [1] mentioned 1921 as the first time that the subsidence phenomenon in Shanghai was reported, and that the problem continued till 1963. A cumulative subsidence of 2.63m was observed with greatest subsidence occurring between 1956 and 1959, at an annual rate of 98mm. A comprehensive study of the land subsidence phenomenon in Shanghai has been provided by [1] and [2]. The relationship connecting groundwater pumping and land subsidence [2], at 6 epochs during the period 1921- 2001, is provided in Fig. 1.

In 1963, some measures including restriction and rational usage of ground water, artificial recharge of ground water, and adjustment of exploited aquifers [1], were put in place to check the subsidence problem. The enforcement of those measures resulted in considerable rebound of water level between 1963 and 1965. The Shanghai Municipal Government in 1995 came out with another policy that limited the usage of underground water of the whole city to less than 10 million cubic meters per year, and also demanded that all deep wells in the city are to operate with official permits [3][4]. In spite of these measures, Shanghai is still experiencing some degree of subsidence. The average land subsidence rates, gathered from Shanghai Geological Survey Institute, are 12.12 mm in 2000, 10.94 mm in 2001, and 10.22 mm in 2002 [3], and the target land subsidence rates as perceived by the Shanghai Municipal Land and Resources Administration Bureau are at most 10 mm by 2005 and 5mm by 2010.

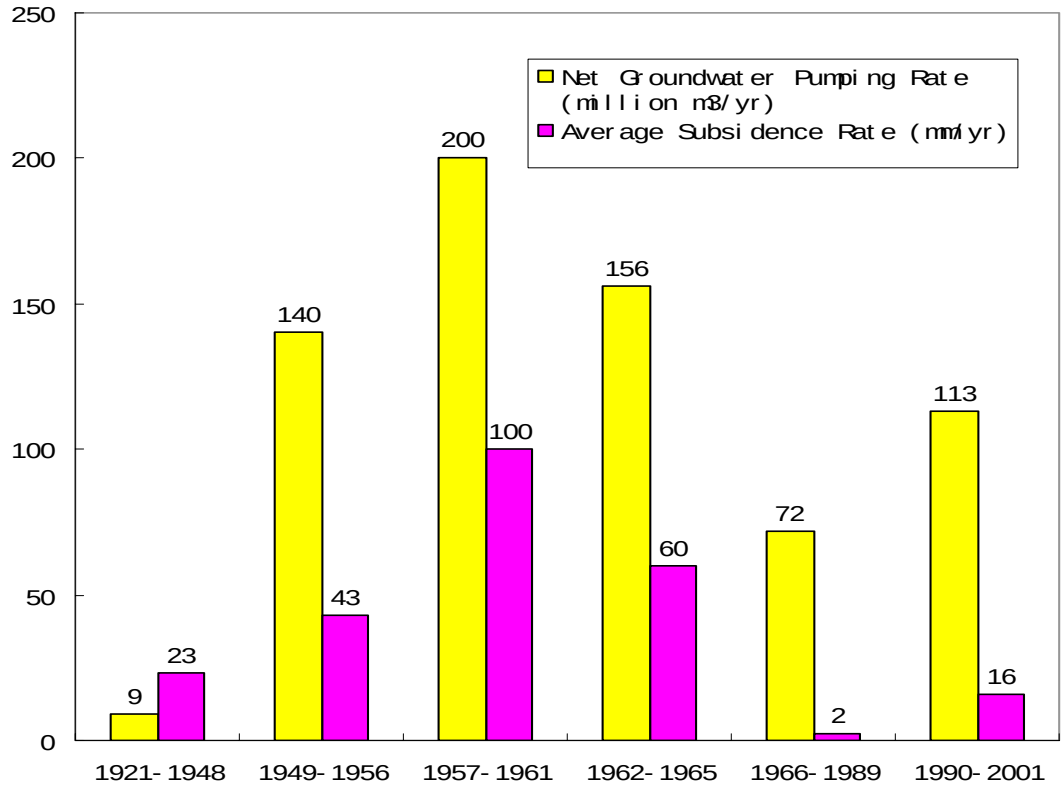

Fig. 1: Relationship between Average Subsidence Rate and Net Groundwater Pumping Rate (Source: [2]).

Subsidence phenomenon in Shanghai has been previously measured or monitored using the surveyor's method of precise leveling, and more recently the GPS. Although these methods provide precise measurements they are labour and time intensive, costly and are restricted to specific points in the terrain. They cannot therefore be used to provide information on detailed ground motions if the area of ground subsidence is large. Inteferometric synthetic aperture radar (InSAR), a method developed by electrical engineers, has demonstrated the capability of mapping extensive areas, on pixel-by-pixel basis, and in a more convenient manner than the aforementioned geodetic methods. InSAR is capable of detecting ground surface elevation changes with centimetric to millimetric precisions [5][6][7]. InSAR distinguishes itself from other precise geodetic techniques with the characteristic that it is a remote sensing tool that requires no presence in the field and is available practically worldwide [7]. Chen et al., [8] argued that InSAR is presently the only technology capable of monitoring the deformation of the Earth's surface in a large area with dense points, quickly and cost-effective, in day and night under all weather conditions.

This study demonstrates the power of the PInSAR technique, a method originally developed by researchers in Politecnico di Milano, Italy, hereafter referred to as Ferretti et al., [9], in deformation measurements. The goal is to employ this relatively new technique to measure the subsidence phenomenon in Shanghai using ERS-1 and ERS-2 SAR SLC scenes acquired over Shanghai in descending orbit during the time period 6 June 1992 – 20 November 2001.

Permanent Scatterer (PS) InSAR Technique

Differential interferometry (DInSAR) has been very useful in many application areas including geophysical and environmental studies. Typical areas where DInSAR has had strong impact include the measurement or monitoring of ground deformation. DInSAR provides users with the capability of mapping and monitoring subtle changes on the ground surface with very high precision in the order of 1 cm or less [6] albeit the main limitations – temporal and geometric decorrelation, and atmospheric inhomogeneities [9][10]. The presence of atmospheric signals, however, in interferograms can limit the accuracy of InSAR measurements [11][12]. Li et al., [11] argue that the level of tropospheric delays in InSAR measurements can introduce decimeter errors to the measured ground displacements and a few hundred meters of errors to the measured terrain height. The length of the normal baseline (i.e., between 30m and 70 m) that is suitable for surface change detection [13] practically limits the exploitation of most ERS-1 and ERS-2 SAR data in the archives for DInSAR applications.

Permanent scatterers (PS) are temporally-stable and highly reflective ground features or phase stable point-wise radar targets [9]. Interferometry using permanent scatterers is a relatively new technique that has demonstrated the capability of measuring ground displacements, to a very high degree of accuracy previously unachievable using

DInSAR [10][14]. The PS InSAR (PSInSAR) technique is gaining popularity as tool for deformation measurements due to its ability to overcome the limitations of the conventional InSAR. The PSInSAR technique was invented by researchers at Politecnico Di Milano (POLIMI) in Italy, in 1999, hereafter referred to as Ferretti et al. [9]. The technique requires the processing of at least 30 differential interferograms [9][10][14] referred to a unique master image over the same place to identify a network of temporally-stable, highly reflective ground features – permanent scatterers. Favourable results, however, have been obtained using fewer numbers of interferograms than the number specified [15][16][17]. The phase history of each scatterer is extracted to provide interpolated maps of average annual ground motion, thus providing a 'virtual' GPS network with 'instant' history.

The main motivation of using permanent scatterers in interferometry for measuring ground displacements is that some terrain features, even in vegetated areas, show consistent backscattering characteristics over time, and hence have good coherence even for intereferograms with baselines exceeding the critical one [10]. An advantage [10] of utilizing these point-wise scatterers (PS) in interferometry for deformation studies is that, it will enable the full exploitation of the ERS SAR data in the ESA archive. Some studies on the theory and the applications of PSInSAR technique have been reported [9][10][14][15][16][17][18][19][20][21][22][23]. A complete treatise of the PSInSAR technique has been provided by [10].

The measurement accuracy of PS depends on number of factors such as [24]: (1) the stability of each PS, (2) the distance of the PS from the reference (calibration) point; (3) the number of images used in the processing; (4) the distribution of images in temporal domain; and (5) the dispersion of normal baseline values. Accuracy increases with increasing numbers of images. Given the same number of images the set with an evenly distribution of temporal baseline and normal baseline will result in higher accuracies than the set of image that is unevenly distributed. It is worthy to point out that the technique works best in urban areas where man-made structures increase the likelihood of finding a non-fluctuating scatterer in any given pixel [23].

Study Area and Data Description

The City of Shanghai and its surroundings are covered by ERS-1 and ERS-2 SAR single look complex (SLC) scenes of Track 3, and Frames 2961 and 2979. Nineteen (19) SAR images from Frame 2979 (Table 1), acquired at an altitude of about 785 km with a mean look angle of 23 during the period June 6, 1992 – November 20, 2001, were used in this study. The images have a maximum relative temporal baseline of 3454 days (approximately 9.5 years) and a minimum relative temporal baseline of 1 day. A Shuttle Radar Topography Mission (SRTM) C-band DEM with resolution of 3 arc-second (90 m) was used as an external DEM in this study to remove the topographic phase from the differential interferograms. The DEM was downloaded freely from the USGS website. Precise orbit data for ERS-1 and ERS-2 were downloaded from the website of the Delft Institute for Earth-oriented Space Research (DEOS) to enable the removal of flat-earth phase from the differential interferograms.

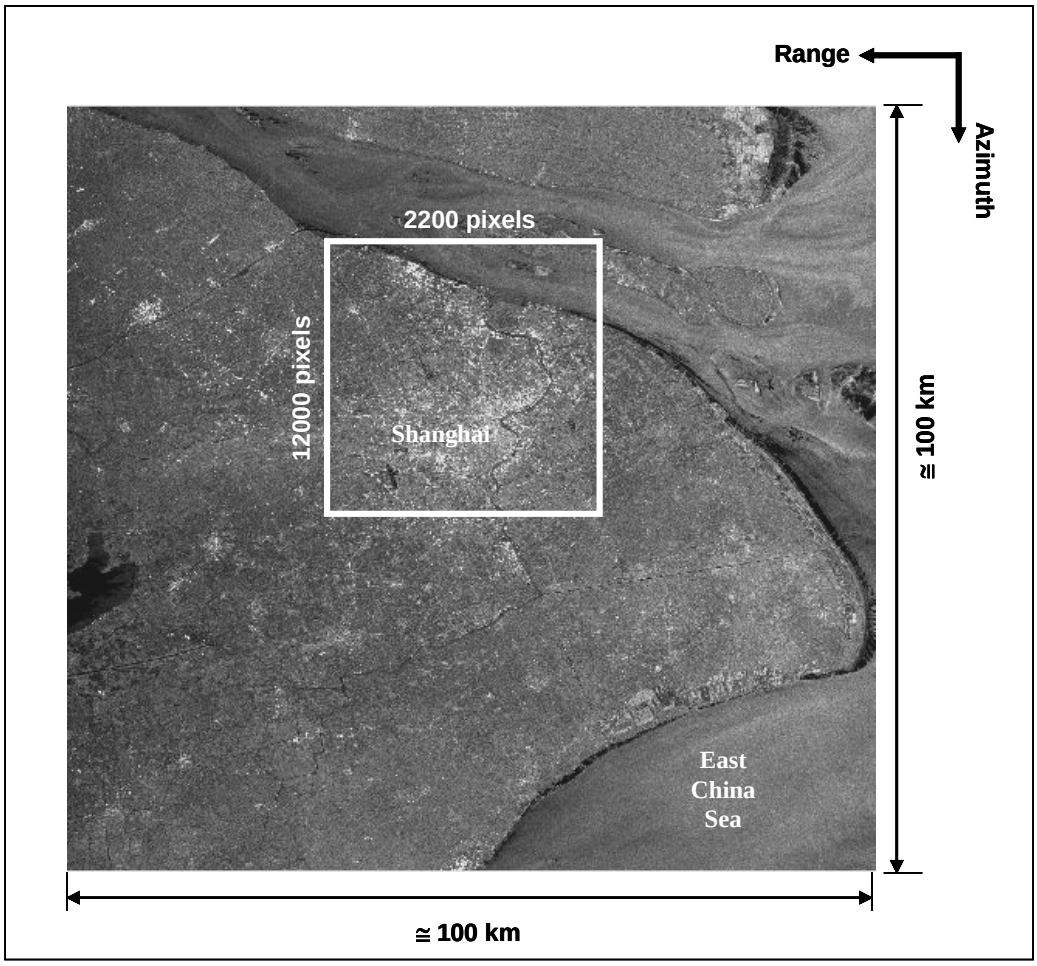

Fig. 2: ERS-2 SAR Intensity image of Track 3 and Frame 2979 acquired on 31/03/1998 over Shanghai. The study area which is made up of 2200 pixels in range direction and 12000 pixels in azimuth direction is marked by the white rectangle.

PS Processing

The Coherent Target Module (CTM) of the EV-InSAR v.3.1 Software, a product of Atlantis Scientific Inc., Canada, was used for the PS processing. The CTM processing is made up of 4 basic stages: data input, interferometric processing, CTM analysis, and product generation. Some key issues to be addressed before and during PS processing include: (1) selection of region of interest (ROI); (2) selection of a suitable Master SAR image; (3) coregistration of all SAR images unto a unique Master image; and (4) selection of a relatively stable area for the estimation and correction of the atmospheric phase screen. A region covering 2200 pixels in the range (across track) direction and 12000 pixels in the azimuth (along track) direction was selected (Fig. 2). All SAR images were coregistered unto a unique master SAR image (ERS-2 05/05/1998) with reliable root mean square (RMS) errors, in both X and Y directions, as shown in Table 1.

The master SAR image was selected based on factors including: the SAR image that forms as many as possible interferometric combinations with the others; an image that minimises the dispersion of normal baseline values; and the date, time and weather conditions during image acquisition. It is expedient to select an image acquired near the centre of the temporal baseline.

Table 1: ERS-1and ERS-2 SAR SLC scenes of Track 3 and Frame 2979 used for the study.

Run ID	Satellite ID	Orbit	Acquisition Date	Normal Baseline (m)	Temporal Baseline (days)	Coregistration RMS (pixels)	
						X	Y
1	ERS-1	04657	06/06/1992	151.848	-2159	0.070	0.082
2	ERS-1	06160	09/19/1992	41.364	-2054	0.047	0.046
3	ERS-1	09166	04/17/1993	89.512	-1844	0.042	0.044
4	ERS-1	10669	07/31/1993	-9.152	-1739	0.046	0.036
5	ERS-1	12172	11/13/1993	-529.422	-1634	0.035	0.042
6	ERS-1	19530	04/10/1995	-458.272	-1121	0.045	0.041
7	ERS-1	22035	10/02/1995	43.868	-946	0.027	0.030
8	ERS-1	24039	02/19/1996	358.060	-806	0.041	0.027
9	ERS-2	04366	02/20/1996	398.898	-805	0.031	0.030
10	ERS-2	15388	03/31/1998	-515.853	-35	0.037	0.039
0	**ERS-2**	**15889**	**05/05/1998**	**0**	**0**	**0.000**	**0.000**
11	ERS-2	20899	04/20/1999	120.115	350	0.035	0.031
12	ERS-2	21400	05/25/1999	-144.961	385	0.026	0.028
13	ERS-2	23905	11/16/1999	-347.993	560	0.047	0.038
14	ERS-2	24406	12/21/1999	-398.013	595	0.037	0.032
15	ERS-2	26410	05/09/2000	357.195	735	0.033	0.040
16	ERS-2	26911	06/13/2000	-467.829	770	0.041	0.036
17	ERS-2	28414	09/26/2000	118.242	875	0.033	0.039
18	ERS-2	34426	11/20/2001	-141.046	1295	0.046	0.050

Results and Discussions

In PS processing, some intermediate products (e.g., unwrapped/atmospheric-corrected differential interferograms, atmospheric delay maps, DEM error and temporal coherence images) are generated in addition to the final products (e.g., deformation map, point profiles, and average backscatter image). Only the unwrapped/atmospheric-corrected differential interferograms, deformation map, and point profiles are presented in this paper.

Differential Interferograms

Fig. 3 shows the 18 differential interferograms processed for the extraction of PS in this study. They are arranged row-wise according to the temporal baseline, starting from the first acquisition in the series. It can be seen that those interferograms with very long temporal baselines are noisy, and that they could not maintain a good level of coherence. It is also evident from the temporal baselines that the SAR images are not evenly distributed in terms of acquisition dates, which in fact can affect the accuracy of the final results.

Deformation Map

Similar to DInSAR technique, the PS technique measures deformation or displacement in the line of sight (LOS) direction of the radar satellite. However, the LOS displacement can be projected into horizontal and vertical components. The displacement phenomenon in Shanghai is known to be one of vertical, hence deformation measurements shown in Fig. 5 is mainly vertical – subsidence (negative values) and upsidence (positive values). A temporal coherence (TC) threshold of 0.78 was used to extract the PS, based on the relationship connecting number scenes and a 4-standard deviation (Sigma) temporal coherence threshold as shown in Fig. 4. Only points having TC values greater than or equal to the specified TC threshold were extracted. As can be seen from Fig. 4, one needs to extract points with TC above 0.73 with 18 interferograms, and a value of 0.78 was used considering the density of PS extracted.

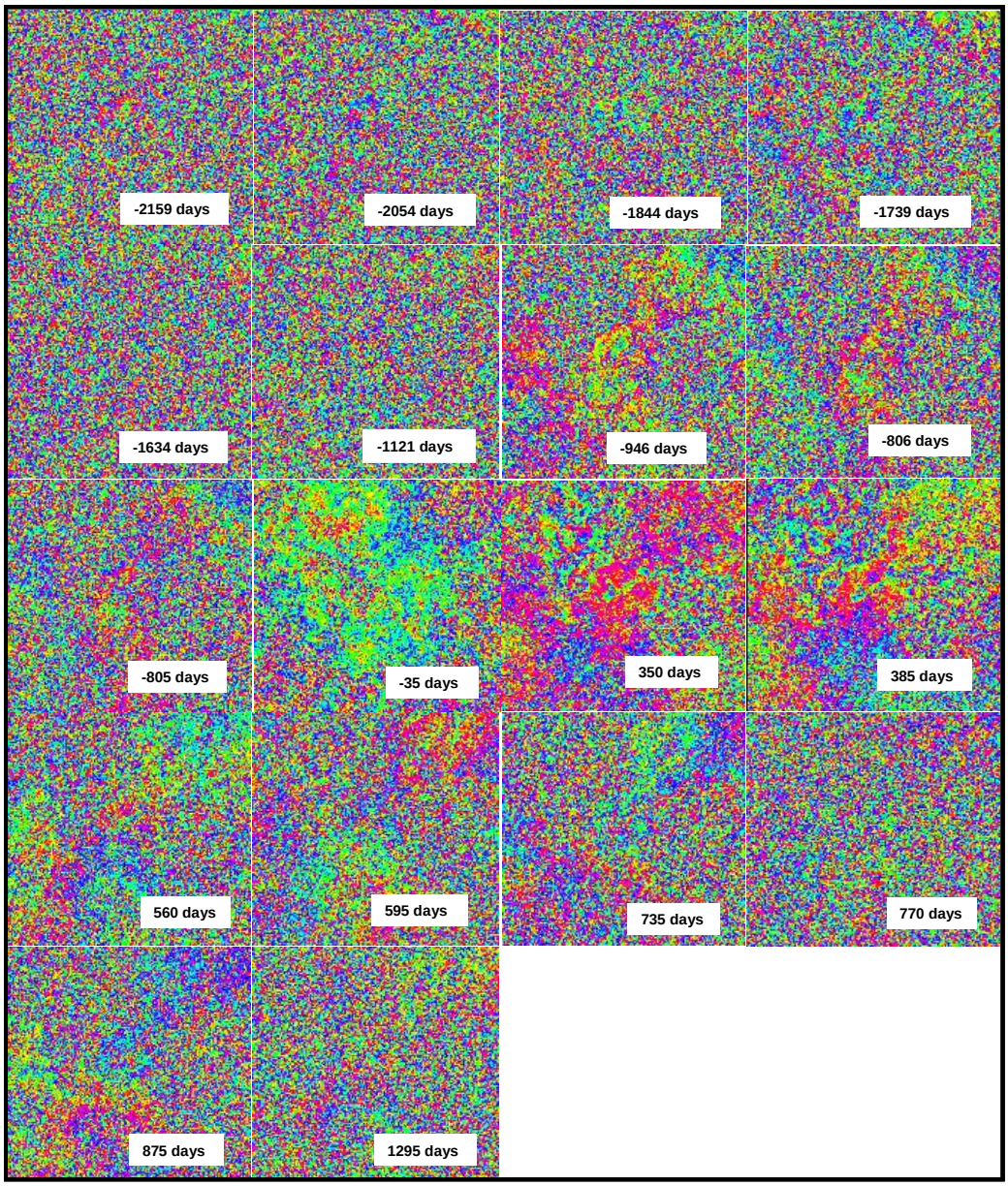

Fig. 3: Differential interferograms processed for the extraction of PS in this study. They have been arranged in rows according to temporal baseline, starting from one acquired first in the series.

A total of 21223 PS were extracted from the region of interest (i.e., 2200 pixels in range direction by 12000 pixels in azimuth direction). Displacement values obtained fall between -12 mm/yr and +1 mm/yr (Fig. 5). This, in fact, is in sympathy with the reported results of Li et al., [17]. They obtained deformation rates ranging between -40 mm/yr and +40 mm/yr, with a large percentage of the values falling in the interval -15mm/yr to +5mm/yr. However, there are some discrepancies in the two results at some regions. Such discrepancies might have resulted due to a number of reasons including: (1) the number of SAR images, (2) the distribution of SAR images with respect to temporal baseline, and (3) the selected master image used in the two studies. For instance, Li et al., [17] used 26 SAR images with the master image acquired on 12/21/1999, but in this study only 19 SAR images were used with the image acquired on 05/05/1998 selected as master.

Another observation made from the deformation map shown in Fig. 5 is that, the PS depicted a regular pattern at some regions whiles at some regions the pattern depicted are not easy to interpret. The pattern depicted in regions C and E, and some parts of regions B and D are regular, and by inspection one can conclude that there is a deformation phenomenon going on at these regions. However, the PS pattern depicted in region A, and parts of regions B and D cannot be interpreted easily. Some reasons that could be suggested for this irregular pattern could be due to the presence of random noise (that could not be minimized or removed during PS processing), and the fact there is no appreciable deformation taking place at these regions (even if there is, the rate is constant and very slow). Fig. 6 shows the point profile or deformation history of a point within region E from 1992 to 2001. It is evident from the graph that the point experienced a linear subsidence of about 70 mm within the 9.5 years interval.

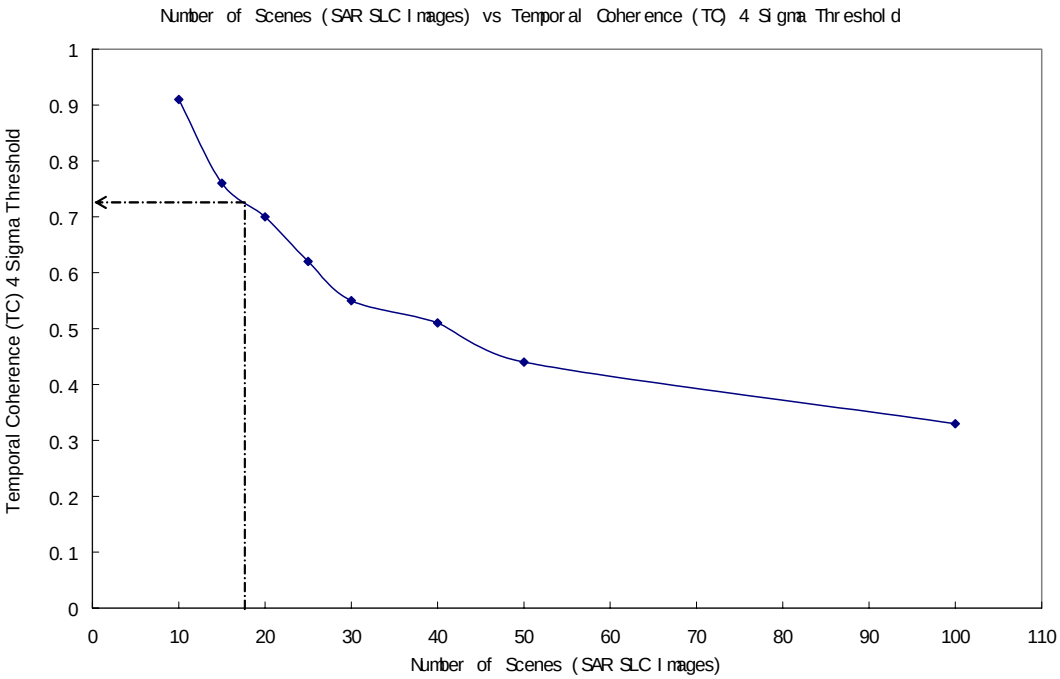

Fig. 4: Temporal Coherence 4-Sigma threshold presented as a function of number of scenes (Source: [25]).

Conclusion

The applicability and effectiveness of using the permanent scatter technique for measuring ground deformation are investigated in this study. Using 19 ERS-1 and ERS-2 SAR images acquired between the period 6 June 1992 and 20 November 2001, deformation rates for a section of Shanghai have been measured with the PS technique. A little more than 21000 PS were extracted with deformation rates falling within the interval -12 mm/yr and + 1 mm/yr. The result obtained is in sympathy with some reported results. Although there were some irregular deformation patterns in the results of this study, there is still some evidence of the strength of the PS technique over traditional methods of measuring ground deformations.

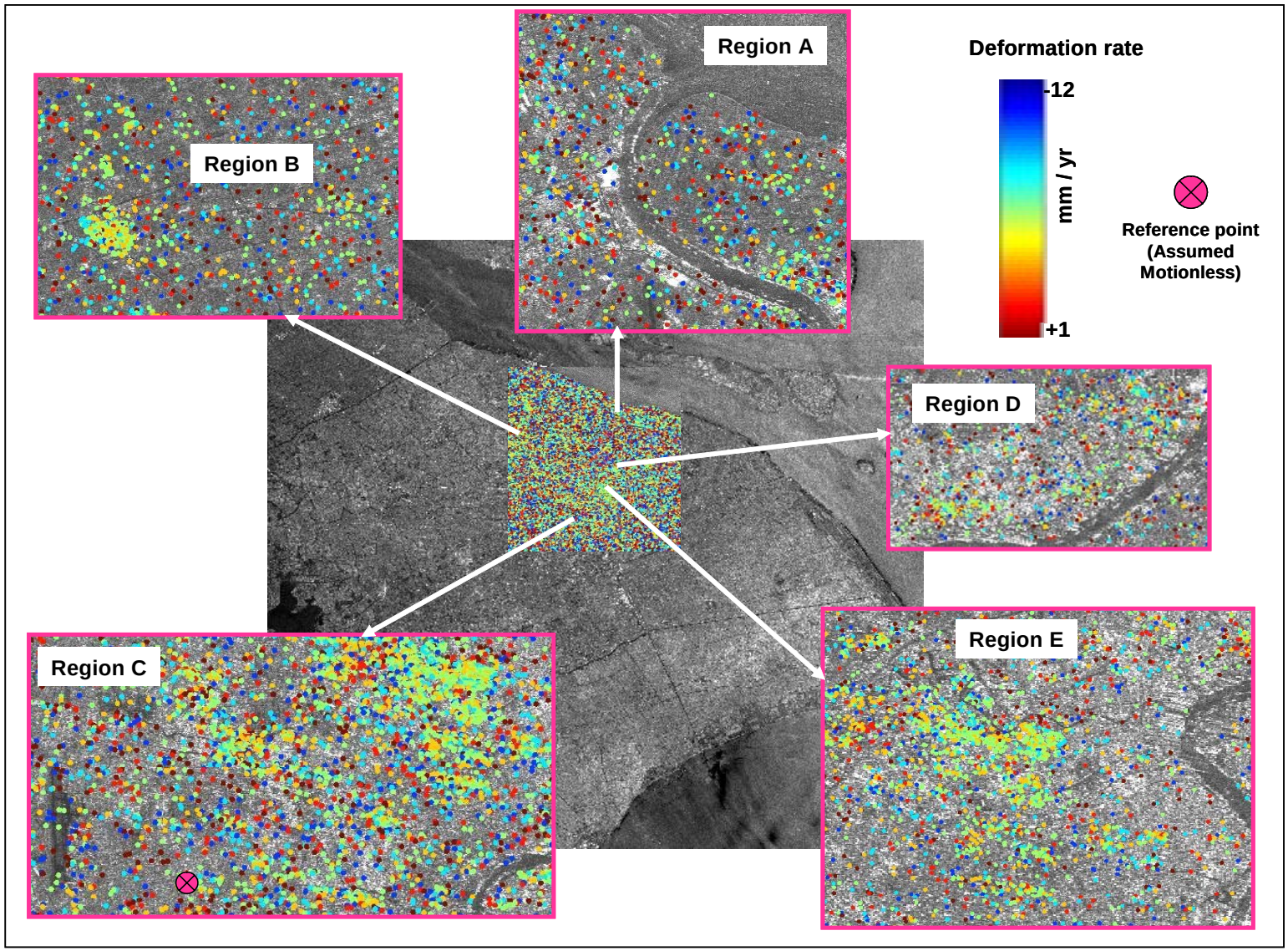

Fig. 5: Deformation map of the study area. Deformation values, after calibration using a reference point, ranges from -12 to +1 mm/yr.

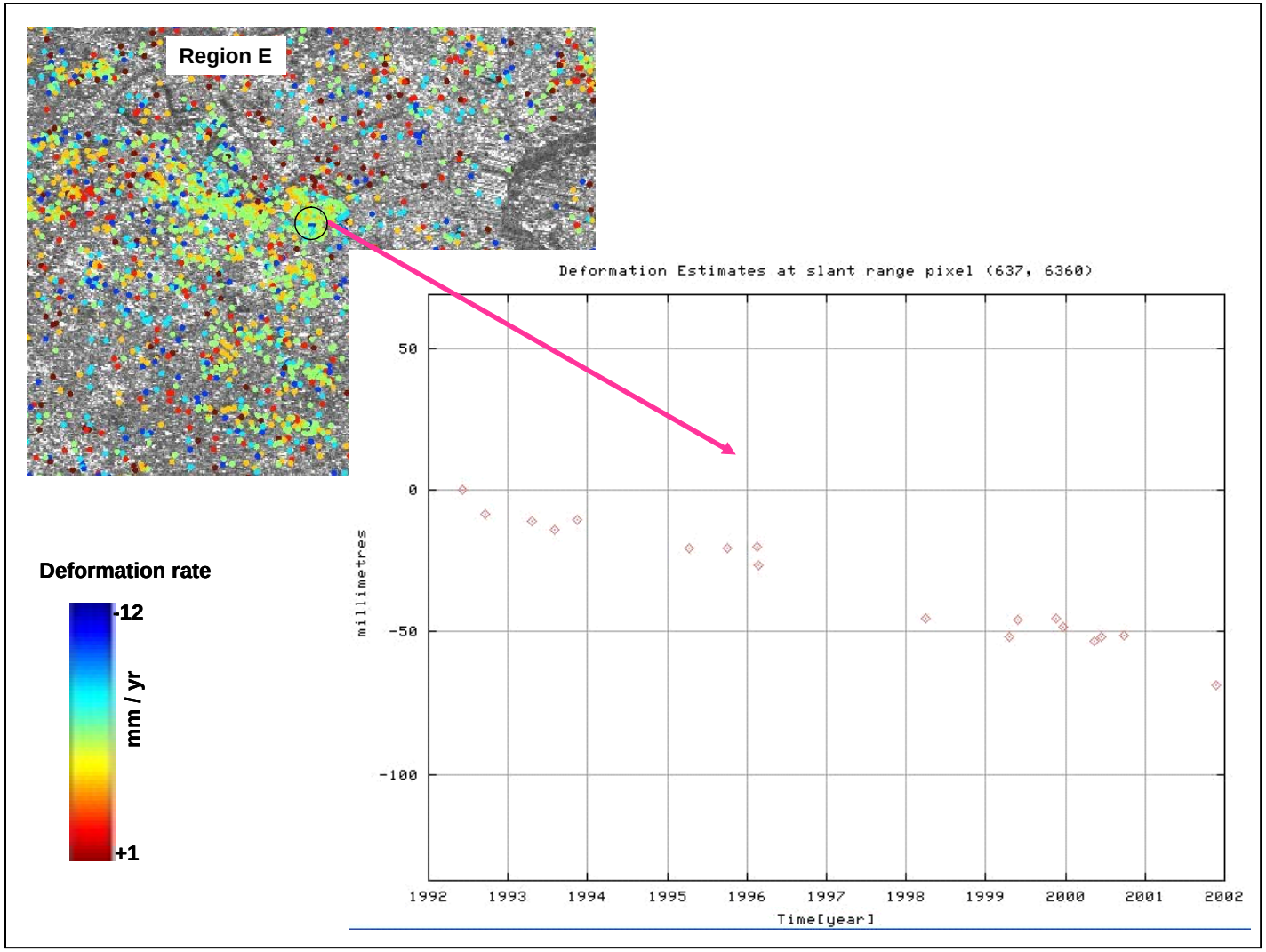

Fig. 6: A zoomed-in of the lower right window (Zone E) of Figure 5, showing the deformation history of the selected point arrowed in the figure.

References

[1]. Shi, L.X. and M.F. Bao, 1984. Case History No. 9.2: Shanghai, China. Guidebook to Studies of Land Subsidence due to Ground-water Withdrawal (J.F. Poland, ed.), UNESCO, Paris. *Available at http://wwwrcamnl.wr.usgs.gov/rgws/Unesco/PDF-Chapters/Chapter9-2.pdf.*

[2]. Chai, J.C., S.L. Shen, H.H. Zhu, and X.L. Zhang, 2004. Land Subsidence due to Groundwater Drawdown in Shanghai. *Géotechnique, 54(2):143-147.*

[3]. **URL:** Shanghai puts up a Fight to Stop Sinking. *ChinaDaily, 16th July 2003.* Available at *http://www2.chinadaily.com.cn/en/doc/2003-07/16/content_245660.htm.*

[4]. **URL:** China Facts and Figures 2002: Shanghai Fights Land Subsidence. *Xinhua News Agency, 10th September 2002.* Available at *http://www.china.org.cn/english/China/42536.htm.*

[5]. Zebker, H.A., 1987. Atmospheric Effects in Interferometric Synthetic Aperture Radar Surface Deformation and Topographic Maps. *Journal of Geophysical Research, 102(B4): 7547-7563.*

[6]. Gabriel, A.K, R.M. Goldstein, and H. A. Zebker, 1989. Mapping Small Elevation Changes over Large Areas: Differential Radar Interferometry. *Journal of Geophysical Research, 94(B7): 9183-9191.*

[7]. Burgmann, R., P.A. Rosen, and F.J. Fielding, 2000. Synthetic Aperture Radar Interferometry to Measure Earth's Surface Topography and its Deformation. *Annual Reviews of Earth and Planetary Sciences, 28:169-209.*

[8]. Chen, Y.Q., G.B. Zhang, X.L. Ding, and Z.L. Li, 2000. Monitoring Earth Surface Deformations with InSAR Technology: Principle and Some critical Issues. *Journal of Geospatial Engineering, 2(1): 3-21.*

[9]. Ferretti, A., C. Prati, and F. Roca, 1999. Permanent Scatterers in SAR interferometry. *IEEE Proceedings on Geoscience and Remote Sensing Symposium, IGARSS'99, June 28 – July 2, 3:1528 -1530.*

[10]. Ferretti, A., C. Prati, and F. Rocca, 2001. Permanent Scatters in SAR Interferometry. *IEEE Transactions on Geoscience and Remote Sensing, 39(1): 8-20.*

[11]. Li, Z.W., X.L. Ding, G.L. Liu, Y.Q. Chen, Z.L. Li, and J.J. Zhu, 2002. Study of Atmospheric Effects on Satellite Synthetic Aperture Rader (SAR) measurements in tropical regions. JS17 Special Sensors and Techniques in Engineering Surveys. *FIG XXII International Congress, April 2002, Washington D.C., USA.*

[12]. Liu G.X., Y.Q. Chen, X.L. Ding, Z.L. Li, and Z.W. Li, 2002. Monitoring Ground Settlement in Hong Kong with Satellite SAR Interferometry. JS17 Special Sensors and Techniques in Engineering Surveys. *FIG XXII International Congress, April 2002, Washington D.C., USA.*

[13]. Solaas, G.A. 1994. ERS-1 Interferometric Baseline Algorithm Verification. *ESA Technical Report S-TN-DPE-OM-GS02, 1994.*

[14]. Ferretti, A., C. Prati, and F. Rocca, 2000. Nonlinear Subsidence Rate Estimation Using Permanent Scatters in Differential SAR Interferometry. *IEEE Transactions on Geoscience and Remote Sensing, 38(5): 2202-2212.*

[15]. Colesanti, C., R. Locatelli, and F. Novali, 2002. Ground Deformation Monitoring Exploiting SAR Permanent Scatterers. *IEEE Proceedings on Geoscience and Remote Sensing Symposium, IGARSS'02, 24-28 June, 2:1219-1221.*

[16]. Fruneau, B., B. Deffontaines, J. Rudant, A. Le Parmentier, C. Colesanti, S. Le Mouelic, C. Carnec, and A. Ferretti, 2003. Conventional and PS Differential SAR Interferometry for Monitoring Vertical Deformation due to Water Pumping: The Haussmann-St-Lazare Case Example (Paris, France). *Proceedings of FRINGE 2003 Workshop, 1-5 December 2003, Frascati, Italy.*

[17]. Li, D. M. Liao, Y. Wang, and T. Wang, 2005. The Application of ESA DATA in Topographic Measurement. *5th Workshop of Asia-Pacific Space Geodynamic Program, 15-17 June 2005, Hong Kong, P.R. China.*

[18]. Colesanti, C. A. Ferretti, C. Prati, and F. Rocca, 2002. Full exploitation of the ERS archive: Multi Data Set Permanent Scatterers Analysis. *IEEE Proceedings on Geoscience and Remote Sensing Symposium, IGARSS'02, 24-28 June, 2:1234-1236.*

[19]. Colesanti, C. A. Ferretti, F. Novali, C. Prati, and F. Rocca, 2003. SAR Monitoring of Progressive and Seasonal Ground Deformation using the Permanent Scatterers Technique. *IEEE Transactions on Geoscience and Remote Sensing, 41(7):1685-1701.*

[20]. Werner, C., U. Wegmuller, T. Strozzi, and A. Wiesmann, 2003. Interferometric Point Target Analysis for Deformation Mapping. *Proceedings of Geoscience and Remote Sensing Symposium, IGARSS'03, 21-25 July, 7: 4362-4364.*

[21]. Worawattanamateekul, J., J. Hoffmann, N. Adam, and B. Kampes, 2003. Urban deformation monitoring in Bangkok metropolitan (Thailand) Using permanent scatterer and differential interferometry techniques. *Proceedings of FRINGE 2003 Workshop, 1-5 December 2003, Frascati, Italy.*

[22]. Adam, N., B. Kampes, M. Eineder, J. Worawattanamateekul, and M. Kircher, 2003. The Development of a Scientific Permanent Scatterer System. *Joint Workshop High Resolution Mapping from Space, Hannover, Germany, 6-8 Octorber, 2003.*

[23]. Hooper, A., H. A. Zebker, P. Segall, and B. Kampes, 2004. A New Method for Measuring Deformation on Volcanoes and other Natural Terrains using InSAR Persistent Scatterers. *Geophysical Research Letters, 31(23), L23611 (DOI 10.1029/2004GL021737).*

[24]. **URL:** Frequently Asked Questions, 2004. *Terrafirma. Pan-European Ground Motion Hazard Information Service. Available at http://www.terrafirma.eu.com/faq.htm.*

[25]. EV-InSAR User Guide version 3.1., (May, 2004). Atlantis Scientific Inc. O*ntario, Canada.*